Copolymers of a New Methacrylate Monomer Bearing Oxime Ester and Ether with Methyl Methacrylate: Synthesis, Characterization, Monomer Reactivity Ratios, and Biological Activity

Ibrahim Erol, Sait Kolu

Department of Chemistry, Faculty of Science and Arts, University of Afyon Kocatepe, Afyonkarahisar, Turkey

Received 11 March 2010; accepted 21 July 2010
DOI 10.1002/app.33090
Published online 13 October 2010 in Wiley Online Library (wileyonlinelibrary.com).

ABSTRACT: The free-radical copolymerization of 2-metil-1-{[(1-{4-[(4-nitrobenzil)oksi]fenil}etilidene)amino]oksi}prop-2-en-1-on (NBOEMA) with methyl methacrylate (MMA) was carried out in 1,4-dioxane at 65 ± 1°C. The copolymers were analyzed by Fourier transform infrared spectroscopy, ^{1}H-NMR, ^{13}C-NMR, and gel permeation chromatography (GPC). Elemental analysis was used to determine the molar fractions of NBOEMA and MMA in the copolymers and for the characterization of the compounds. The monomer reactivity ratios were calculated according to the general copolymerization equation with the Kelen–Tudos and Fineman–Ross linearization methods. The polydispersity indices of the polymers, determined with GPC, suggested a strong tendency for chain termination by disproportionation. The thermal behaviors of the copolymers with various compositions were investigated by differential scanning calorimetry and thermogravimetric analysis. The glass-transition temperature of the copolymers increased with increasing NBOEMA content in the copolymers. Also, the apparent thermal decomposition activation energies were calculated by the Ozawa method with a Shimadzu TGA 60H thermogravimetric analysis thermobalance. All of the products showed moderate activity against different strains of bacteria and fungi. The photochemical properties of the polymers were investigated by UV spectroscopy. © 2010 Wiley Periodicals, Inc. J Appl Polym Sci 120: 279–290, 2011

Key words: activation energy; biomaterials; copolymers; differential scanning calorimetry (DSC); FT-IR

INTRODUCTION

Functional groups give a polymer structure a special character substantially different from the inherent properties of the basic polymer chain.[1] In recent years, some comprehensive work has been published on functional monomers and their polymers.[2] Methacrylic polymers find extensive applications in fiber optics, metal complexes, polymeric reagents, and polymeric supports.[3–7] Recent investigations have been reported on the use of oxime esters as irreversible acyl-transfer agents.[8] This methodology has been used elegantly for the preparation of chiral polymers[9] and regioselective acylation of nucleosides and to obtain various nucleoside derivatives of medicinal significance.[10] In a previous article,[11] methacrylate-containing oxime ester was used as an irreversible acyl-transfer agent. Athawale et al.[12,13] synthesized geranyl methacrylate and (±) MMA by a transesterification reaction using 2,3-butane dione monooxime methacrylate as an acylating agent. *O*-Acyloximes can be used as photobase generators, and they have been proven to be quite efficient.[14–19]

Crown ethers, macrocyclic polyethers with a hydrophobic ethylenic ring surrounding a hydrophilic cavity of ether oxygen atoms, are able to selectively bind a range of inorganic and organic ions and neutral species,[20–22] but their greatest affinity is for alkali and alkaline earth cations.[23] Small and hydrated metal ions become large and lipophilic as crown ether complexes provide increased metal-salt solubility and increased anion reactivity in aprotic organic solvents; this is widely used in studies of mediated ion transport, solute separations, and anion-activated catalysis.[24,25] The polymers with bearing ethers are the types of high-performance polymers that have excellent mechanical and thermal properties. These polymers and their copolymers have found many implementation in the aerospace, coatings, and insulating materials fields.[26,27]

The incorporation of different chemical groups in macromolecular chains can be accomplished by a copolymerization reaction between two different monomers. Knowledge of the copolymer composition

Correspondence to: I. Erol (ierol@aku.edu.tr or iberol@hotmail.com).

Contract grant sponsor: Afyon Kocatepe University Research Fund; contract grant number: 08-FENED-12.

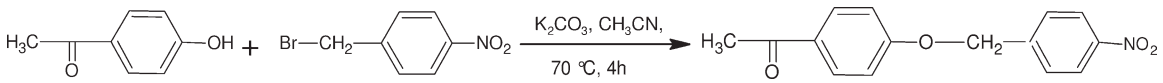

Scheme 1 Synthesis of 1-{4-[(4-nitrobenzyl)oxy]phenyl}ethanone.

is an important step in the evaluation of its utility. The copolymer composition and its distribution depend on the monomer reactivity ratios. The most common mathematical model of copolymerization is based on the determination of the relationship between the composition of the copolymers and the composition of the monomer feed in which the monomer reactivity ratios are the parameters to be determined.[28,29] The calculation of the monomer reactivity ratios requires the mathematical treatment of experimental data of the composition of the copolymers and the monomer in the feed mixtures. The most fundamental quantity characterizing a copolymer is its composition on a molar basis, which is eventually used for the determination of the relevant monomer reactivity ratios. Spectroscopic methods, preferably ^{1}H-NMR and ^{13}C-NMR spectroscopy,[30,31] and elemental analysis are probably the most widely used methods for analyzing copolymers and determining the reactivity ratios.

Thermogravimetric analysis (TGA) has been widely used to investigate the decomposition characteristics of many materials. Some methods have already been established to evaluate the kinetic parameters from thermogravimetric data.[32,33]

No studies on the reactivity ratios in the copolymerization of 2-metil-1-{[(1-{4-[(4-nitrobenzil)oksi]fenil}etilidene)amino]oksi}prop-2-en-1-on (NBOEMA) with any commercial monomer were found in the literature. NBOEMA is a new methacrylate monomer bearing oxime ester and aryl ether groups. In this article, the results of the radical copolymerization of NBOEMA with methyl methacrylate (MMA), the determination of the monomer reactivity ratios with elemental analysis, the effects of the copolymer composition/thermal behavior relationships, and an investigation of the biological activity properties are presented and discussed.

EXPERIMENTAL

Materials

1,4-Dioxane, chloroform, methanol, and ethanol (Merck, Germany) were freshly distilled over molecular sieves before use. Methacryloyl chloride, 4-hydroxyacetophenon, and 4-nitrobenzyl bromide (Merck, Germany) were used as received. MMA was freed from the inhibitor by washing with a 5% NaOH solution and then distilled water, drying over anhydrous $MgSO_4$, and distillation *in vacuo*. 2,2′-Azobisisobutyronitrile (AIBN) was recrystallized from a chloroform–methanol (1 : 1) mixture.

Measurements

Infrared spectra were obtained with a PerkinElmer spectrum BX Fourier transform infrared (FTIR) (California, USA) spectrometer with KBr pellets in the 4000–400-cm^{-1} range, and 10 scans were taken at a 4-cm^{-1} resolution. ^{1}H-NMR and ^{13}C-NMR spectra in dimethyl sulfoxide (DMSO) solutions were recorded on a Bruker GmbH DPX-400 400 MHz FT-NMR spectrometer (Leipzig, Germany) with tetramethylsilane as an internal reference. The molecular weights of the polymer were determined with a Waters 410 gel permeation chromatograph equipped with a refractive-index detector and calibrated with polystyrene standards. Thermal data were obtained with a Shimadzu DSC-60H (Tokyo, Japan) instrument at a heating rate (β) of 10°C/min and with a Labsys TGA thermobalance at a heating rate (β) of 20 C/min in an N_2 atmosphere. Elemental analyses were carried out with a Elementar CHNS (Germany) microanalyzer.

Solubility studies

The solubility values of the homopolymers and copolymers were tested via the mixing of 10 mg of each polymer with 5 mL of various solvents in test tubes. After the closed tubes were set aside for 1 day, the solubility was observed. The homopolymers and copolymers were soluble in 1,4-dioxane, dimethyl acetamide, dimethyl formamide, DMSO, and tetrahydrofuran (THF) but were insoluble in *n*-hexane, *n*-heptane, ethanol, and methanol solvents.

Synthesis of the 1-{4-[(4-nitrobenzyl)oxy]phenyl}ethanone

The reaction type between *p*-hydroxyacetophenon and 4-nitrobenzylbromide is a nucleophilic substitution. A solution of *p*-hydroxyacetophenon (1 mol) and K_2CO_3 (1 mol) in anhydrous acetonitrile (20 mL) was used for the preparation of 1-{4-[(4-nitrobenzyl)oxy]phenyl}ethanone. To the solution was added dropwise 4-nitrobenzylbromide (1 mol). The reaction mixture was stirred at 70°C, for 4 h. After the reaction, 1-{4-[(4-nitrobenzyl)oxy]phenyl}ethanone was crystallized from ethanol.

Yield = 84%. IR (neat, cm^{-1}): 1700 (C=O for carbonyl), 1610 (aromatic C=C), 1250 ($PhCH_2$—O—C).

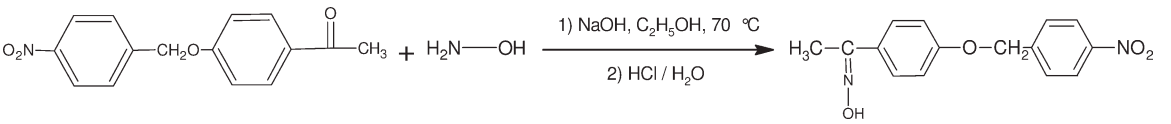

Scheme 2 Synthesis of *N*-hydroxy-1-{4-[(4-nitrobenzyl)oxy]phenyl}ethanimine.

The reaction paths are shown in Scheme 1.

Synthesis of *N*-hydroxy-1-{4-[(4-nitrobenzyl)oxy]phenyl}ethanimine

N-Hydroxy-1-{4-[(4-nitrobenzyl)oxy]phenyl}ethanimine was synthesized according to a standard method.[34] The synthesis route is shown in Scheme 2.

Yield = 86%. ANAL. Calcd: C, 62.93%; H, 4.93%; N, 9.79%. Found: C, 62.72%; H, 4.80%; N, 9.75%. IR (neat, cm^{-1}): 3300–3400 (OH stretching for oxime), 1610 (aromatic C=C), 1250 ($PhCH_2$—O—Ph), 3100 (aromatic C—H).

Monomer synthesis

The synthesis of the monomer is shown in Scheme 3. The synthesis of NBOEMA was performed as follows: *N*-hydroxy-1-{4-[(4-nitrobenzyl)oxy]phenyl} ethanimine (1 mol) and K_2CO_3 (1 mol) were dissolved in 20 mL of CH_2Cl_2 at 0°C, and then, methacryloyl chloride (1.1 mol) was added dropwise to the solution. The reaction mixture was stirred at room temperature for 24 h. The organic layer was washed several times with diethyl ether and dried over $MgSO_4$. After the diethyl ether was removed, 2-metil-1-{[(1-{4-[(4 nitrobenzil)oksi]fenil}etilidene)amino]oksi}prop-
2-en-1-on (NBOEMA) was crystallized from ethanol.

Yield ≈ 82%. ANAL. Calcd: C, 64.40%; H, 4.19%; N, 7.91%. Found: C = 64.35%; H, 5.10%; N, 4.24%. IR (KBr, cm^{-1}): 1775 (methacrylic carbonyl), 1635 (CH_2=C—), 1600 (C=C), 1500 (C=N), 1254 ($PhCH_2$—O—Ph). ^{1}H-NMR (δ, ppm, from tetra methyl silan (TMS) in $CDCl_3$): 7.0–8.3 (aromatic protons, 8H), 5.6 (CH_2=, 1H), 6.2 (CH_2=, 1H), 5.3 (—OCH_2—, 2H), 2.3 (—N=CCH_3, 3H), 1.9(—CH_3,3H). ^{13}C-NMR (δ, ppm, from TMS in $CDCl_3$): 169.0 (C=O of esters), 130.0 (=C), 129.1 (CH_2=), 114.1–159.8 (aromatic carbons), 65.0 (—OCH_2—), 16.5 (N=CCH_3), 18 (CH_3).

Polymerization of the NBOEMA monomer

The polymerization of NBOEMA was carried out in glass ampules under an N_2 atmosphere in a 1,4-dioxane solution with AIBN (1% on the basis of the total weight of the monomers) as an initiator. The reacting components were degassed by threefold freeze–thawing cycles and then immersed in an oil bath at 65°C for a given reaction time. The polymers were separated by precipitation in *n*-hexane and reprecipitated from a 1,4-dioxane solution. The polymers were finally dried *in vacuo* to a constant weight at room temperature and kept in a desiccators *in vacuo* until use.

Copolymerization

The copolymerizations of NBOEMA with MMA at five different feed compositions were carried out in 1,4-dioxane at 65°C with AIBN (1% on the basis of the total weight of the monomers) as an initiator. Appropriate amounts of NBOEMA with MMA and 1,4-dioxane were mixed in a polymerization tube, purged with N_2 for 20 min, and kept at 65°C in a thermostated water bath. The reaction time (~ 2.5 h) was selected to give conversions of less than 10 wt % to satisfy the differential copolymerization equation. The conversion of the monomer to the polymer was

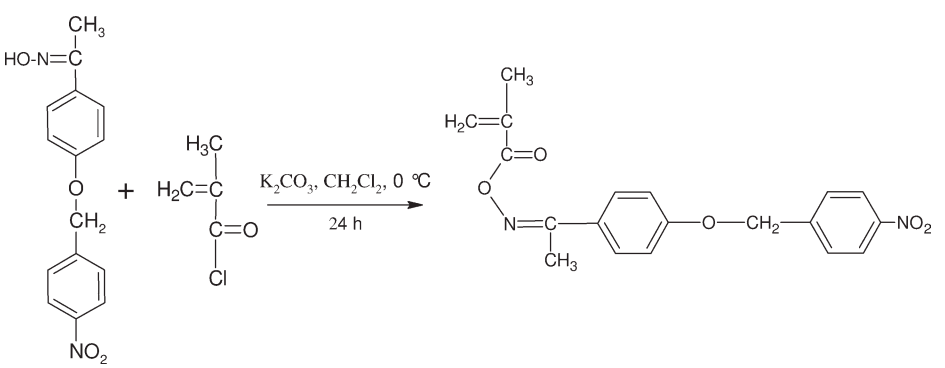

Scheme 3 Synthesis of the NBOEMA monomer.

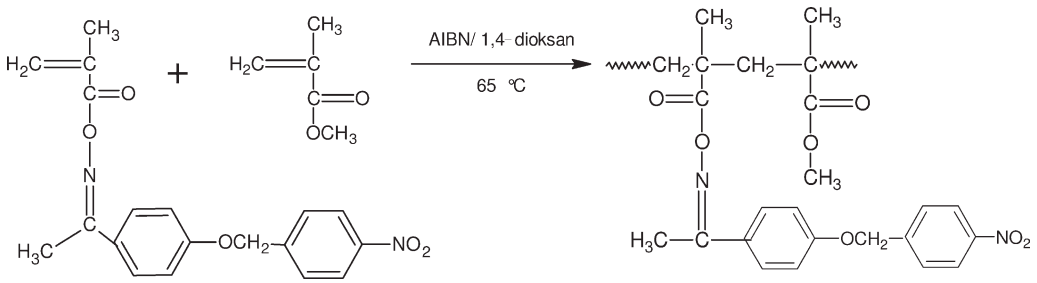

Scheme 4 Synthesis of the poly(NBOEMA-*co*-MMA).

determined by the gravimetric method. After the desired time, the copolymerization was stopped. These copolymers were poured into excess ethanol to precipitate, filtered, purified by repeated reprecipitation from a solution of each polymer in 1,4-dioxane by ethanol, and dried in a vacuum oven at 50°C to a constant weight. The amounts of monomeric units in the copolymers were determined by elemental analysis benefiting from N content of NBOEMA units. The syntheses of the copolymers are shown in Scheme 4.

RESULTS AND DISCUSSION

Structural characterization of the poly(2-metil-1-{[(1-{4-[(4-nitrobenzil)oksi]fenil}etilidene)amino]oksi}prop-2-en-1-on) [poly(NBOEMA)]

Some characteristic absorption peaks in the FTIR spectrum of the poly(NBOEMA) were at 1760 cm^{-1} (oxime carbonyl stretching) and 1252 cm^{-1} ($PhCH_2$—O—Ph stretching). During the polymerization of the monomers, the IR band at 1635 cm^{-1} (C=C) disappeared, and oxime ester carbonyl stretching for polymers shifted to about 1760 cm^{-1}. The main evidence of the polymer was certainly the disappearance of some characteristic signals of the double bond in the spectra, and this fact was effectively observed in our case. Thus, two bands vanished in the IR spectrum: the absorption band at 923 cm^{-1} assigned to the C—H bending of geminal $=CH_2$ and the stretching vibration band of C=C at 1600 cm^{-1}. The ^{1}H-NMR and ^{13}C-NMR spectra of the poly(NBOEMA) are presented in Figure 1; these were in good agreement with the structure. From ^{1}H-NMR spectroscopy, the formation of the polymer was also clearly evident from the disappearance of two singlets at 5.6 and 6.2 ppm of the vinyl protons and the appearance of broad signals at 1.5 and 2.2 ppm assigned to an aliphatic $-CH_2-$ group. In the proton-decoupled ^{13}C-NMR spectrum of poly (NBOEMA), chemical shift assignments were made from the off-resonance decoupled spectra of the polymer. The resonance signals at 172 ppm corresponded to the oxime ester group present in the polymer. The aromatic carbons were observed at 115–160 ppm. The α-methyl group of the polymer showed resonance signals at 19 ppm.

Characterization of the copolymers

The copolymerization of NBOEMA with MMA in the 1,4-dioxane solution was studied in a wide composition interval with the molar fractions of NBOEMA ranging from 0.1 to 0.7 in the feed. The reaction time was selected in the trials to give conversions of less than 10% to satisfy the differential copolymerization equation.

Solubility parameters (δ's)

The polymers were soluble in chloroform, dimethylformamide, DMSO, THF, and dichloromethane but were insoluble in *n*-hexane, *n*-heptane, and

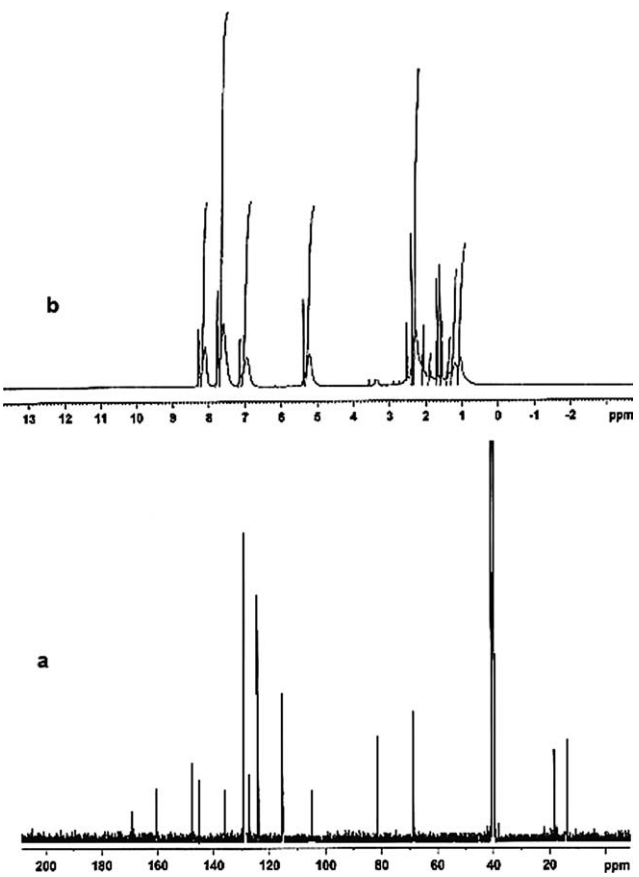

Figure 1 (a) ^{13}C-NMR and (b) ^{1}H-NMR spectra of poly(NBOEMA).

TABLE I
Monomer Compositions in the Feed and in the Copolymer

Sample	Feed composition (molar fraction)		δ	Conversion		Copolymer composition (molar fraction)	
	NBOEMA (M_1)	MMA (M_2)	$(cal/cm^3)^{1/2}$	(%)	N (%)	NBOEMA (m_1)	MMA (m_2)
1	0.10	0.90	9.53	8.50	1.63	0.07	0.93
2	0.30	0.70	9.62	7.80	4.10	0.23	0.77
3	0.40	0.60	9.71	7.30	5.50	0.35	0.65
4	0.50	0.50	9.80	8.70	5.95	0.46	0.54
5	0.70	0.30	9.84	9.00	6.70	0.62	0.38

hydroxyl-group-containing solvents, such as methanol and ethanol. The δ values of the copolymers were between 9.53 and 10.25 $(cal/cm^3)^{1/2}$. These values were close to 9.53 $(cal/cm^3)^{1/2}$, which was δ of THF. THF was the best solvent for all of the copolymers. The δ values are presented in Table I.

Spectroscopic characterization

The FTIR spectrum of the copolymer, poly(2-metil-1-{[(1-{4-[(4-nitrobenzil)oksi]fenil}etilidene)amino]oksi} prop-2-en-1-on-*co*-methyl methacrylate) [poly (NBOEMA-*co*-MMA)] (0.07 : 0.93), is shown in Figure 2. The band at 1675 cm^{-1} (—C=N stretching in the NBOEMA units) was the most characteristic for the copolymer. The peak at 3050 cm^{-1} corresponded to the C—H stretching of the aromatic system. Symmetrical and asymmetrical stretching due to the methyl and methylene groups was observed at 1985, 2940, and 2865 cm^{-1}. The shoulder at 1745 cm^{-1} and a peak at 1765 cm^{-1} were attributed to the ester and oxime ester carbonyl stretching of the MMA and NBOEMA units, respectively. Ring breathing vibrations of the aromatic nuclei were observed at 1600, 1505, and 1470 cm^{-1}. The asymmetrical and symmetrical bending vibrations of methyl groups were seen at 1455 and 1380 cm^{-1}. The C—H and C—C out-of-plane bending vibrations of the aromatic nuclei were observed at 790 and 565 cm^{-1}, respectively. The ^{1}H-NMR spectrum of poly(NBOEMA-*co*-MMA) was consistent with its chemical structure. The chemical shifts assignments for the copolymers were based on the chemical shifts observed for the respective homopolymers. The aromatic protons showed signals between 7.25 and 8.37 ppm. The spectrum showed one signal at 5.24 ppm due to the —OCH_2 group. The methyl protons attached to the azomethine nuclei gave a signal centered at 2.41 ppm. Because of the existence of tacticity, the resonance signals corresponding to the methylene group of the polymer backbone were observed between 1.91 and 1.45 ppm. The α-methyl groups of the NBOEMA and MMA units showed resonance signals at 1.20 and 0.97 ppm, respectively.

The proton-decoupled ^{13}C-NMR spectrum of poly (NBOEMA-*co*-MMA) (0.35 : 0.65) is shown in Figure 3. The resonance signals at 178.56 and 176.21 ppm belonged to the ester carbonyl carbons of the NBOEMA and MMA units. The signals at 70 ppm were due to the —OCH_2 carbons of the NBOEMA unit. The aromatic carbon attached to the oxygen atom showed a signal at 145.21 ppm. The other aromatic carbons gave signals at 125.60 and 128.45 (C12 and C13), 115.98 (C7 and C8), and 138.20 ppm (C14). The methyleneoxy (C11) group gave a signal at 68.20 ppm. The signals due to the backbone methylene

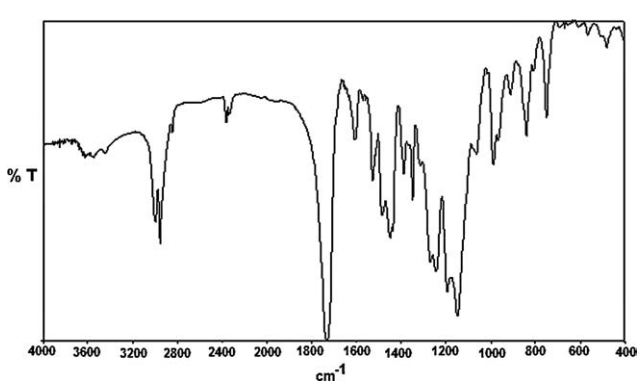

Figure 2 FTIR spectrum of poly(NBOEMA-*co*-MMA) (0.7 : 0.93).

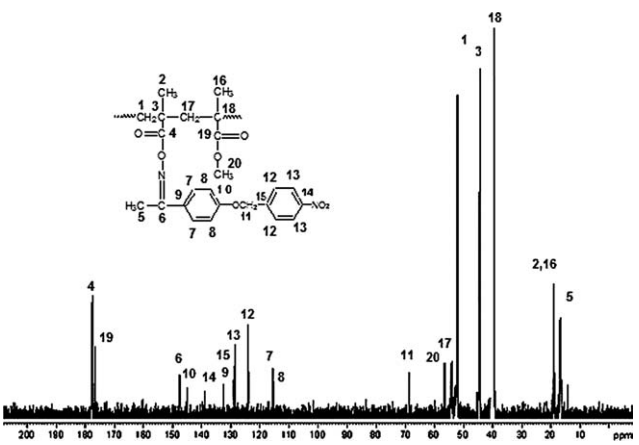

Figure 3 ^{1}H-NMR spectrum of poly(NBOEMA-*co*-MMA) (0.35 : 0.56).

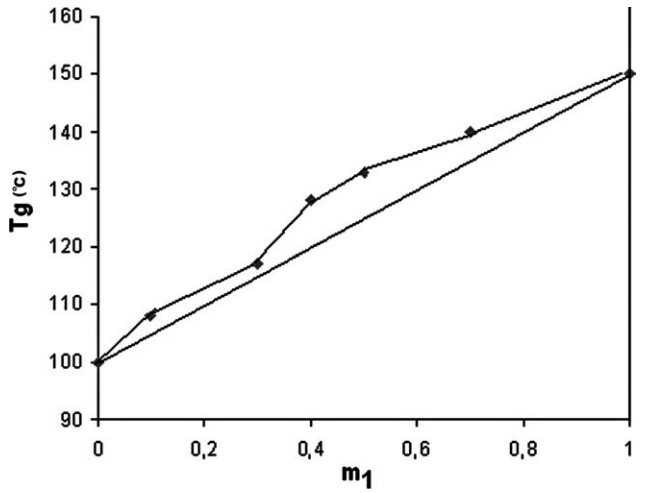

Figure 4 Variation of T_g (°C) with the composition of the poly(NBOEMA-*co*-MMA) system.

and tertiary carbon atoms were observed at 52.10 and 45.70 ppm, respectively. The methyl groups attached to the azomethine (C=N) nuclei showed a signal at 15.54 ppm. The α-methyl group of both monomer units showed a resonance at 18.50 ppm.

Copolymer compositions

The number of monomeric units in the copolymers was determined by elemental analysis. The results are presented in Table I.

Glass-transition temperatures (T_g's)

The T_g values were determined with a Shimadzu 60 differential scanning calorimeter. Samples of about 5–8 mg held in sealed aluminum crucibles at β of 10°C/min under a dynamic nitrogen flow (5 L/h) were used for the measurements. From the differential scanning calorimetry measurements, T_g was taken as the midpoint of the transition region. T_g of poly(NBOEMA) was 150°C, and that of poly(methyl methacrylate) [poly(MMA)] was 100°C. Among the many strategies available for increasing the T_g of methacrylate polymers, the most promising is the replacement of the methyl group in the ester part of the monomer. Sterically hindered and conformationally rigid cycloalkyl groups cause a significant increase in T_g. For example, T_g varies from 110°C for poly(cyclohexyl methacrylate) to 194°C for poly (bornyl methacrylate) and 200°C for poly(isobornyl methacrylate). Similarly, an increase in the polarity of the ester group causes an increase in T_g, which is observed in 4-cyanophenyl methacrylate (T_g = 155°C). In comparison to that of poly(MMA), the shift to higher temperature was also noted for all of the copolymers studied, and the magnitude of the shift was dependent on the increase in the NBOEMA molar fraction in the copolymer chain. An increase in T_g of the copolymers may have been due to the introduction of NBOEMA into MMA in the comonomer, which increased the intermolecular polar interactions among the molecular chains due to structural stretching. The observed T_g increased with increasing NBOEMA and presented a striking positive deviation with respect to linearity; this was associated with lower free volume, mobility, and flexibility than those in a mixture of MMA and NBOEMA units. The variation of T_g of the copolymers with molar fraction of the NBOEMA unit in the copolymer is shown in Figure 4.

Molecular weights of the polymers

The molecular weights of the polymers were determined by gel permeation chromatography (GPC) with polystyrene and THF as the standard solvents, respectively. The weight-average molecular weight (M_w) and number-average molecular weight (M_n) values and polydispersity indices (M_w/M_n) of the polymer samples are presented in Table II. Both molecular weights decreased with increasing percentage of NBOEMA in the feed composition. This was ascribed to the lower reactivity ratio of this monomer in the copolymerization. GPC traces of the copolymers are shown in Figure 5. The polydispersity index of the copolymers ranged from 1.73 to 1.81. The theoretical values of M_w/M_n for the polymers produced via radical recombination and disproportionation were 1.5 and 2.0, respectively.[35] In the homopolymerization of NBOEMA, the growing chains were terminated by disproportionation. The polydispersity indices of poly(NBOEMA) and poly (MMA) suggested that in both cases, chain termination by disproportionation outweighed coupling, and the tendency for termination by disproportionation was greater for NBOEMA than for MMA. The values of M_w/M_n in copolymerization are also known to depend on chain termination in the same way as in homopolymerization.[36]

TABLE II
Molecular Weights and Polydispersity Index of the Polymers

Sample	$M_w \times 10^4$	$M_n \times 10^4$	M_w/M_n
Poly(NBOEMA)	7.25	4.20	1.72
Poly(MMA)	9.13	5.45	1.67
Poly(NBOEMA-*co*-MMA)			
7/93	8.75	4.90	1.78
23/77	7.80	4.50	1.73
35/65	7.50	4.18	1.79
46/54	7.25	4.10	1.77
62/38	6.55	3.60	1.81

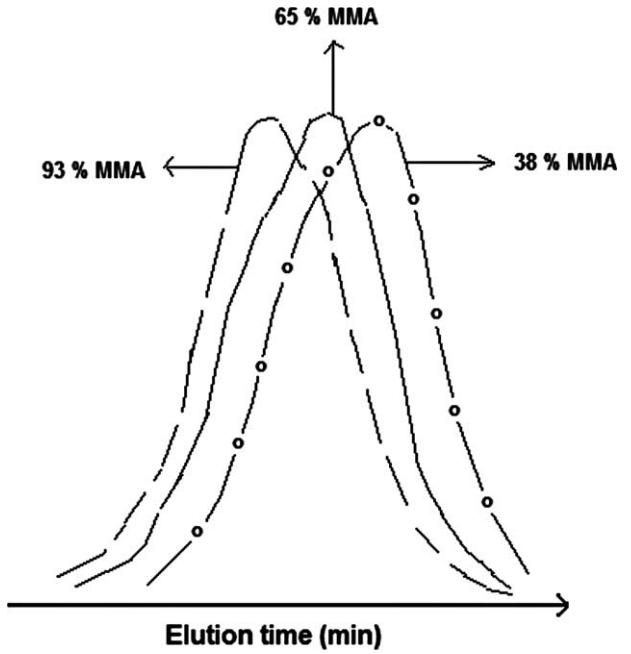

Figure 5 GPC traces of the some copolymers (with THF as an eluent, 0.3 mL/min).

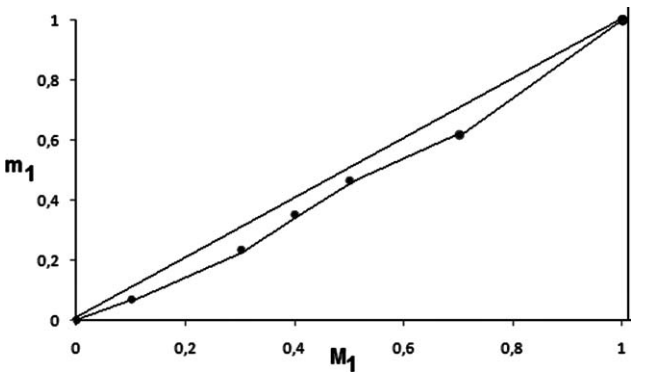

Figure 6 Copolymer composition diagram of poly (NBOEMA-*co*-MMA).

Determination of the monomer reactivity ratios

The monomer reactivity ratios for the copolymerization of NBOEMA with MMA were determined from the monomer feed ratios and the copolymer composition. The plot of the molar fraction of NBOEMA in the feed (M_1) versus that of NBOEMA in the copolymer (m_1) is shown in Figure 6. The Fineman–Ross (FR)[37] and Kelen–Tudos (KT)[38] methods were used to determine the monomer reactivity ratios. The significance of the parameters of the FR and KT equations are presented in Table III. According to the FR method, the monomer reactivity ratios (r_1 and r_2) can be obtained as follows:

$$G = Hr_1 - r_2 \tag{1}$$

where r_1 and r_2 correspond to the reactivity ratios of the NBOEMA and MMA monomers, respectively. The parameters G and H are defined as follows:

$$G = F/(f-1)/f \quad \text{and} \quad H = F^2/f \tag{2}$$

with

$$F = M_1/M_2 \quad \text{and} \quad f = m_1/m_2 \tag{3}$$

where M_1 and M_2 are the monomer molar compositions in the feed and m_1 and m_2 are the copolymer molar compositions.

Alternatively, the reactivity ratios can be obtained with the KT method, which is based on the following equation:

$$\eta = (r_1 + r_2/\alpha)\xi - r_2/\alpha \tag{4}$$

where η and ξ are functions of the parameters G and H:

$$\eta = G/(\alpha + H) \quad \text{and} \quad \xi = H/(\alpha + H) \tag{5}$$

where α is a constant equal to $(H_{max} \times H_{min})^{1/2}$, where H_{max} and H_{min} are the maximum and minimum H values, respectively, from the series of measurements. From a linear plot of η as a function of ξ, the values of η for $\xi = 0$ and $\xi = 1$ can be used to calculate the reactivity ratios according to the following equations:

$$\xi = 0 \rightarrow \eta = -r_2/\alpha \quad \text{and} \quad \xi = 1 \rightarrow \eta = r_1 \tag{6}$$

The graphical plots concerning the methods previously reported are given in Figure 7(a,b), whereas

TABLE III
FR and KT Parameters for the Poly(NBOEMA-*co*-MMA) Systems

Sample number	$F = M_1/M_2$	$f = m_1/m_2$	$G = F(f-1)/f$	$H = F^2/f$	$\eta = G/(\alpha + H)$	$\varepsilon = H/(\alpha + H)$
1	0.111	0.073	−1.410	0.169	−1.521	0.182
2	0.429	0.302	−0.952	0.609	−0.726	0.446
3	0.667	0.542	−0.564	0.821	−0.357	0.520
4	1.000	0.866	−0.155	1.155	−0.081	0.603
5	2.330	1.598	0.872	3.397	0.210	0.818

$\alpha = (H_{max} \times H_{min})^{1/2} = 0.758$.

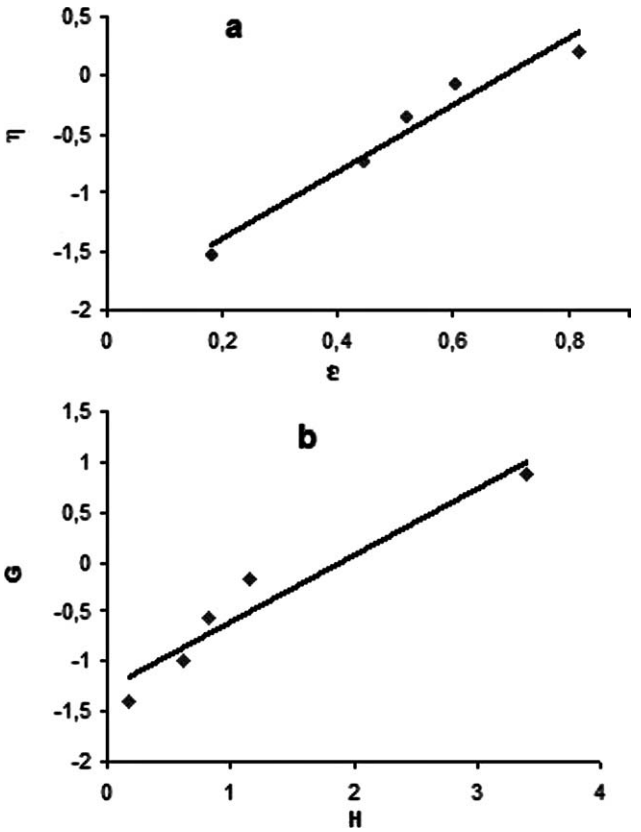

Figure 7 KT and FR plots for the poly(NBOEMA-*co*-MMA) system.

the reactivity ratios are summarized in Table IV. In all cases and for all graphical methods, the plots were linear, and this indicated that these copolymerizations followed conventional copolymerization kinetics and that the reactivity of a polymer radical was determined only by the terminal monomer unit.

The difference between the reactivity ratio values obtained by the FR and KT methods was negligible. The reactivity ratio of MMA ($r_2 = 1.38$) was greater than 1, and that of NBOEMA ($r_1 = 0.78$) was less than 1. The reactivity of growing radicals with the NBOEMA unit, as measured by $1/r_2$, seemed to be higher toward the MMA monomer than toward its own monomer. The r_1 and r_2 values strongly suggested that the copolymer chain contained a greater number of MMA units and fewer NBOEMA units than in the feed. Because the value of r_1 was less than one and the value of r_2 was greater than one, this suggests the presence of a lower amount of NBOEMA units in the copolymer than in the feed. However, product of $r_1 \times r_2$ was greater than one, which indicated that the system led to a random distribution of monomer units with a longer sequence of MMA units in the copolymer chain.

TABLE IV
Copolymerization Parameters for the Free-Radical Copolymerization of NBOEMA with MMA[a]

Method	r_1	r_2	r_1r_2	$1/r_1$	$1/r_2$
FR	0.67	1.27	0.85	1.49	0.79
KT	0.88	1.48	1.30	1.14	0.68
Average	0.78	1.38	1.08	1.28	0.72

[a] r_1 and r_2 are the monomer reactivity ratios for NBOEMA and MMA, respectively.

Decomposition kinetics

The thermal stabilities of the polymers were investigated by TGA in a nitrogen stream at a β of 20°C/min. In Figure 8, the TGA thermograms of the polymers are shown. The degradation of poly(NBOEMA) occurred in three stages. The first stage was observed at 220–280°C. The second-stage decomposition commenced at 320–380°C, and the last stage was observed at 415–450°C. The copolymers with 65, 54, and 38% MMA decomposed in a single stage; the other copolymers decomposed in three stages. The actual decomposition temperature range of the two stages and the initial decomposition temperature of the copolymers depended on the copolymer composition, and the initial decomposition temperature shifted toward higher temperatures with increasing MMA content. The thermal degradation of poly(*n*-alkyl methacrylate)s typically produces the monomer as a result of depolymerization. The formation of cyclic anhydride type structures by intramolecular cyclization is another main process in the degradation of these polymers. The latter produces some low-molecular-weight products, depending on the chemical structures of the side chain of poly(methacrylic ester)s. For the study of the kinetics of the thermal degradation of polymers, one can select isothermal thermogravimetry (ITG) or thermogravimetry (TG) at various β values.[39] ITG is superior for obtaining an accurate activation energy for thermal degradation, although it is time-consuming. For the

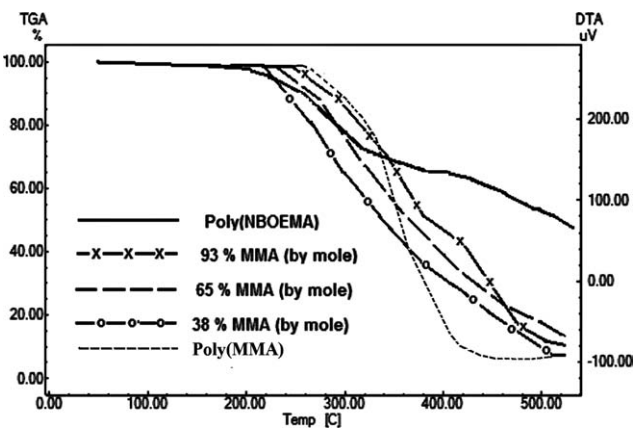

Figure 8 TGA curves for poly(NBOEMA-*co*-MMA) and some copolymers.

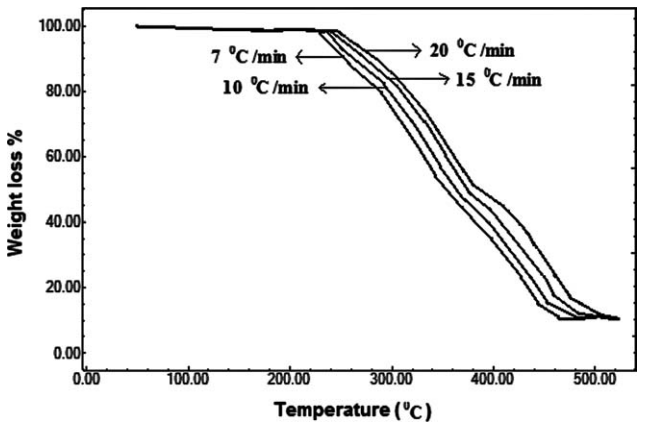

Figure 9 Thermal degradation curves of poly(NBOEMA-*co*-MMA) (0.07 : 0.93) at different β values.

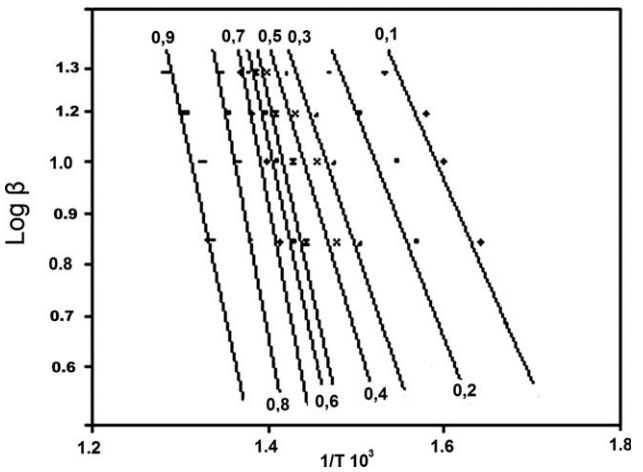

Figure 10 Ozawa's plots of log β versus the reciprocal temperature ($1/T$) at different conversions for poly (NBOEMA-*co*-MMA) (0.35 : 0.65).

thermal degradation of polymers in which depolymerization is competing with cyclization or crosslinking due to the side groups, TG at various β values is much more convenient than ITG for the investigation of the thermal degradation kinetics. Therefore, in this study, we obtained TG curves at β values, and the activation energies for the thermal degradation of the polymers were calculated with Ozawa plots, which are widely used. Degradations were performed in the scanning mode from 35 to 500°C under a nitrogen flow (20 mL/min) at various β values (7.0, 10.0, 15.0, and 20.0°C/min). In Figure 9, the TGA thermograms of poly(NBOEMA-*co*-MMA) (0.07 : 0.93) are shown. Samples (5–8 mg) held in alumina open crucibles were used, and their weights were measured as a function of the temperature, and the results were stored in a list of data of the appropriate built-in program of the processor. The TGA curves were immediately printed at the end of each experiment, and the weights of the sample at various temperatures were then transferred to a personal computer.

According to the method of Ozawa,[40] the apparent thermal decomposition activation energy (E_d) can be determined from the TGA thermograms at various β values, such as those in Figure 10, with the following equation:

$$E_d = -\frac{R}{b}\left[\frac{d\log\beta}{d(1/T)}\right] \quad (7)$$

where R is the gas constant, b is a constant (0.4567), and β is the heating rate (°C/min). According to eq. (7), E_d can be determined from the slope of the linear relationship between log β and the reciprocal of the temperature, as shown in Figure 10. The E_d values for the polymers are given in Table V. E_d calculated from the Ozawa method is superior those calculated by other methods for complex degradation because it does not use the reaction order in the calculation of E_d.[41] Therefore, E_d calculated from the Ozawa method is superior to the former methods for complex degradation.

Antimicrobial screening

The biological activities of the monomers and their homopolymers and copolymers were tested against different microorganisms with DMSO as the solvent. The sample concentrations were 100 μg. All microorganism strains were obtained from the Culture Collection of Microbiology Laboratory of Afyon Kocatepe University (Afyon, Turkey). In this study, *Staphylococcus aureus* ATCC 29213, *Escherichia coli* ATCC 25922, *Pseudomonas aeruginasa* ATCC 27853, *Proteus vulgaris, Salmonella enteridis*, and *Klebsiella pneumoniae* were used as bacteria. *Candida albicans* CCM 31 was a fungus. A Yeast Extract Peptone Dextrose (YEPD) medium cell culture was prepared as

TABLE V
Apparent Activation Energies of the Investigated Copolymers Under Thermal Degradation in N_2

Sample	10	20	30	40	50	60	70	80
Poly(NBOEMA)	98.5	94.8	88.1	81.2	—	—	—	—
Poly(NBOEMA 7%-*co*-MMA)	95.4	93.7	111.2	103.0	113.3	95.8	111.6	121.1
Poly(NBOEMA 35%-*co*-MMA)	93.6	91.0	91.2	101.4	105.3	89.8	98.1	101.6
Poly(NBOEMA 62%-*co*-MMA)	88.7	85.7	86.8	99.1	100.8	85.1	91.8	99.7

TABLE VI
Antimicrobial Effects of the Compounds (mm of Zones)

Compound	*P. aeruginasa*	*E. coli*	*P. vulgaris*	*S. enteridis*	*K. pneumoniae*	*S. aureus*	*C. albicans*
NBOEMA	16	14	16	16	15	17	16
Poly(NBOEMA)	13	13	13	14	12	14	15
Poly(NBOEMA-*co*-MMA)							
7/93	11	11	10	12	9	10	11
23/77	12	13	12	—	—	11	—
35/65	—	—	13	—	11	13	14
46/54	13	14	14	13	13	14	15
62/38	14	15	—	15	—	15	—
Penicillin G	16	16	9	16	18	17	35
Teicoplanin	18	18	11	22	25	12	15
DMSO	—	—	—	—	—	—	—

Compound concentration = 100 μg/disc. The em dash (—) reveals that the compounds had some activity against the microorganisms.

described by Connerton.[42] YEPD medium (10 mL) was inoculated into each cell from plate cultures. Yeast extract (1% w/v), bactopeptone (2% w/v), and glucose (2% w/v) were obtained from Difco. The microorganisms were incubated at 35°C for 24 h. About 1.5 mL of these overnight stationary-phase cultures were inoculated into 250 mL of YEPD and incubated at 35°C until OD_{600} reached 0.5.

The antibiotic sensitivity of the polymers was tested with an antibiotic disk assay, as described previously.[43] Nutrient agar was purchased from Merck. About 1.5 mL of each prepared different cell culture was transferred into 20 mL of nutrient agar and mixed gently. The mixture was inoculated into the plate. The plates were rotated firmly and allowed to dry at room temperature for 10 min. Prepared antibiotic discs (50 and 100 μg) were placed on the surface of the agar medium.[44] The plates were kept at 5°C for 30 min and then incubated at 35°C for 2 days. If a toxic compound leached out from the disc, that indicated that the microbial growth was inhibited around the sample. The width of this area expressed the antibacterial or antifungal activity by diffusion. The zones of inhibition of microorganism growth of the standard sample monomers, homopolymers, and copolymers were measured with a millimeter ruler at the end of the incubation period.

The results were standardized against penicillin G and teicoplanin under the same conditions. All of the compounds exhibited moderate activity comparable to that of the standard drugs. The NBOEMA monomer and its homopolymer were the most effective in inhibiting the growth of the microorganisms; this may have been due to the high oxime ester and ether contents of these compounds. As the percentage of MMA in the copolymer increased, the effectiveness of the copolymers at inhibiting the growth of the microorganisms decreased. The data reported in Table VI are the average data of three experiments. The results show that the investigated polymers had good biological activity, comparable to that of standard drugs such as penicillin G and teicoplanin. The results suggest that the monomers and polymers and some copolymers had good biological activity against *S. aureus* microorganisms in comparison with standard drugs.

UV spectra of the polymers (Fig. 11)

A solution of poly(NBOEMA) and copolymers in DMSO was cast onto a quartz glass plate with a spin coater and was then annealed for 30 min at 40°C. The thin film (0.8–1 μm) was irradiated with a fixed energy of light from a Spex Fluorolog 2 with a 450-W xenon lamp. Figures 6 compares the absorption spectra of the polymers, and the following

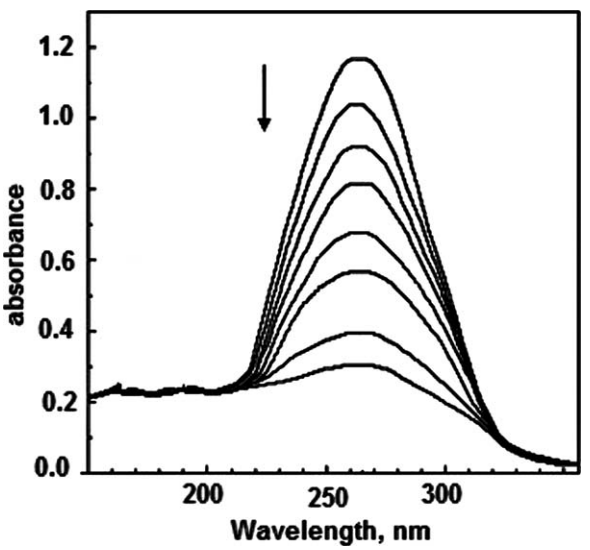

Figure 11 UV–vis absorption spectra of poly(NBOEMA-*co*-MMA) (0.23 : 0.77) in DMSO (irradiation times = 0, 1, 2, 3, 6, 10, 12, 15, and 20 min).

includes the absorption characteristics in the UV spectra. The UV spectra of the polymers showed an absorption maxima at 250 nm for poly(NBOEMA) and one at about 255 nm for copolymers due to the π–π* transition of C=C (phenyl) and C=N of the pendant oxime ester group chromophore present in the polymer unit. The absorption spectrum of poly (NBOEMA) suggested that the energy states of the chromophore substituted by two phenyl groups differed somewhat from those of other chromophores. In fact, we anticipated that the chromophore interactions in these polymers would have been suppressed between the C=N groups attached in the vicinity of each chromophore group, such as ester. The absorption properties were only slightly affected by the ester group. This was attributed to a $S_0 \rightarrow S_1$ transition localized on the oxime moiety. Because of their structural analogy and the presence of an electron lone pair on the heteroatom, ketones are often compared with the corresponding oximes,[45] the question being the nature of the electronic transitions. The transition observed for these oxime ester polymers was of π–π* nature, and the presence of a lone pair on the nitrogen atom did not lead to any observable *n*-π* transition.

To obtain more information about the UV stability of the polymers, we investigated the structural changes of the oxime ester chromophore in each copolymer. For the poly(NBOEMA-*co*-MMA) solution, the absorption maxima were centered at about 275 nm. Figure 9 presents a typical example for the change in the UV absorption curve during photodecomposition. The oxime ester chromophore absorption band at 275 nm decreased with irradiation time. In addition, although all of the polymers were soluble in CH_2Cl_2, $CHCl_3$, 1,4-dioxane, and so forth before irradiation, none one of the polymers was soluble in any solvent. All of the experimental data indicated that photodegradation in the oxime ester region occurred and followed crosslinking. The dissociation of oxime led to iminyl radicals and acyloxyl radicals ($RCO_2\cdot$). If the decarboxylation was not fast enough, these two radicals could recombine to give the starting oxime, and therefore, the global efficiency of the photodissociation decreased.[46] On the contrary, the occurrence of the decarboxylation process led to the formation of carbon dioxide and a new radical (R·). The latter could also react in-cage with the iminyl radical to form an imine, which resulted in a decrease in the free iminyl radical quantum yield. Similar results were obtained for the other NBOEMA–MMA copolymers. The polymers reacted photochemically according to a mechanism similar to that found for *O*-acyloximes and its derivatives.[47] Although practical evaluation from the spectral data was rather dubious because the sensitivity of photocrosslinkable polymers is a function of the T_g, molecular weight, polymer solubility, and so on, the discrimination of the photoresponsibilities of the chromophores themselves was possible to a certain extent.

CONCLUSIONS

The synthesis of new methacrylate monomers (NBOEMA) with pendant oxime ester and ether moieties have been reported for the first time. The structures of the monomer and its polymer were characterized by spectroscopic methods. Copolymers of NBOEMA with MMA were prepared by free-radical polymerization in 1,4-dioxane at 65°C. The reactivity ratios of the copolymers were estimated with linear graphical methods. The r_2 values were higher than the corresponding r_1 values in all cases, and this means that a kinetic preference existed for the incorporation of MMA in the copolymer structure. The values strongly suggested that the growing radicals of both monomeric ends preferentially added to the MMA monomer; this led to the formation of a copolymer with a higher amount of MMA. GPC data implied that the polydispersity index of the copolymers was nearly equal to 2, and this implied a strong tendency for chain termination by disproportionation. E_d of the investigated polymers was calculated by the Ozawa method with the TGA data. The polymers had good biological activity, which was comparable to that of standard drugs such as penicillin G and teicoplanin. Finally, the photocrosslinking behavior of the polymers as thin films was tested in the presence of UV light. The increasing utility of photosensitive polymers in many applications, such as microelectronics, printing, and UV-curable lacquers and inks, has provided us with an incentive to obtain novel polymers.

The authors are indebted to Zeki Gürler for the biological activity studies.

References

1. Kim, B. Y.; Ratcliff, E. L.; Armstrong, N. R.; Kowalewsk, T. Pyun, J. Langmuir 2010, 26, 2083.
2. Yactine, B.; Ratsimihety, A.; Ganachaud, F. Polym Adv Technol 2010, 21, 139.
3. Fresvig, T.; Ludvigsen, P.; Steen, H.; Reikeras, O. Med Eng Phys 2008, 30, 104.
4. Ishio, M.; Terashima, T.; Ouch M. I.; Sawamoto, M. Macromolecules 2010, 43, 920.
5. Erol, I.; Soykan, C. React Funct Polym 2003, 56, 147.
6. Erol, I. J Fluorine Chem 2008, 129, 613.
7. Koga, Y.; Matsubara, K. J Polym Sci Part A: Polym Chem 2009, 47, 4358.
8. Ghogare, A.; Kumar, S. J Chem Soc Chem Com 1989, 1533.
9. Ghogare, A.; Kumar S. J Chem Soc Chem Com 1989, 134.
10. Moris, F.; Gotor, V. J Org Chem 1993, 58, 653.
11. Athawale, V.; Manjrekar, N. J Mol Catal B 2000, 10, 551.

12. Athawale, V.; Manjrekar, N.; Athawale, M. J Mol Catal B 2001, 16, 169.
13. Athawale, V.; Manjrekar, N.; Athawale, M. Tetrahedron Lett 2002, 43, 4797.
14. Suyama, K.; Shirai, M. Prog Polym Sci 2009, 34, 194.
15. Suyama, K.; Nakao, S.; Shirai, M. J Photopolym Sci Technol 2005, 18, 141.
16. Ohba, T.; Nakai, D.; Suyama, K.; Shirai, M. J Photopolym Sci Technol 2004, 17, 11.
17. Lalevee, J.; Allonas, X.; Fouassier, J. P.; Tachi, H.; Izumitani, A.; Shirai, M.; Tsunooka, M. J Photopolym Sci Technol 2002, 151, 27.
18. Chae, K. H. Macromol Rapid Commun 1998, 19, 1.
19. Shirai, M.; Endo, M.; Tsunooka, M. J Photopolym Sci Technol 1999, 12, 669.
20. Gokel, G. Crown Ethers and Cryptands; Royal Society of Chemistry: Cambridge, England, 1991; p 64.
21. Lehn, J.-M. Supramolecular Chemistry; VCH: Weinheim, 1995.
22. Rodriguez, J. D.; Kim, D.; Tarakeshwar, P.; Lisy, J. M. J Phys Chem A 2010, 114, 1514.
23. Steed, J. W. Coord Chem Rev 2001, 215, 171.
24. Stark, C. M.; Liotta, C. L. Phase Transfer Catalysis—Principles and Techniques; Academic: New York, 1978.
25. Izatt, R. M.; Christensen, J. J. Process in Macrocyclic Chemistry; Wiley-Interscience: New York, 1981; Vol. 1; 1982, Vol. 2.
26. Çakmak, M. Plast Eng Sci 1997, 41, 931.
27. Jar, P. Y.; Plummer, C. Adv Thermoplast Compos 1993, 111.
28. Arshady, R.; Kenner, G. W.; Ledwith, A. Macromol Chem Phys 1981, 182, 41.
29. Ham, G. Copolymerization; High Polymers Interscience: New York, 1964; Vol. 18.
30. Liang, K.; Dossi, M.; Moscatelli, D.; Hutchinson, R. A. Macromolecules 2009, 42, 7736.
31. Rajendrakumar, K.; Dhamodharan, R. Eur Polym J 2009, 45, 2685.
32. Houchin, M. L.; Topp, E. M. J Appl Polym Sci 2009, 114, 2848.
33. Konaganti, V. K.; Madras, G. Polym Degrad Stab 2009, 94, 1325.
34. Prabhu, V. A.; Brown, R. G.; Delgado, J. N. J Pharm Sci 1981, 70, 558.
35. Teramachi, S.; Hasegawa, A.; Akatsuka, M.; Yamashita, A.; Takemoto, N. Macromolecules 1978, 11, 1206.
36. Melville, H. W.; Noble, B.; Watson, W. F. J Polym Sci 1949, 4, 629.
37. Fineman, M.; Ross, S. D. J Polym Sci 1950, 5, 259.
38. Kelen, T.; Tudos, F. J Macromol Sci Chem 1975, 9, 1.
39. Wendlandt, W. W. Thermal Analysis; Wiley: New York, 1986; p 57.
40. Ozawa, T. Bull Chem Soc Jpn 1965, 38, 1881.
41. Regnier, N.; Guibe, C. Polym Degrad Stab 1997, 55, 165.
42. Connerton, I. F. In Analysis of Membrane Proteins; Gould, G. W., Ed.; Portland: London, 1994; p 177.
43. Chan, E. C. Z.; Pelczar, M. J.; Krieg, N. R. In Laboratory Exercises in Microbiology; Chan, et al.; McGraw-Hill: New York, 1993; p 225.
44. Desai, J. A. J Macromol Sci Pure Appl Chem 1996, 33, 1113.
45. Yoshida, M.; Sakuragi, H.; Nishimura, T.; Ishikawa, S. I.; Tokumaru, K. Tetrahedron Lett 1975, 1125.
46. McCarroll, A. J.; Walton, J. C. J Chem Soc Perkin Trans 2000, 2, 2399.
47. Shirai, M.; Endo, M.; Tsunooka, M. J Photopolym Sci Technol 1999, 12, 669.